Clinical Cancer Research

Overcoming BET Inhibitor Resistance in Malignant Peripheral Nerve Sheath Tumors

Jonathan M. Cooper[1], Amish J. Patel[1,2], Zhiguo Chen[1], Chung-Ping Liao[1], Kun Chen[1], Juan Mo[1], Yong Wang[1], and Lu Q. Le[1,3,4,5]

Abstract

Purpose: BET bromodomain inhibitors have emerged as a promising therapy for numerous cancer types in preclinical studies, including neurofibromatosis type 1 (NF1)-associated malignant peripheral nerve sheath tumor (MPNST). However, potential mechanisms underlying resistance to these inhibitors in different cancers are not completely understood. In this study, we explore new strategy to overcome BET inhibitor resistance in MPNST.

Experimental Design: Through modeling tumor evolution by studying genetic changes underlying the development of MPNST, a lethal sarcoma with no effective medical treatment, we identified a targetable addiction to BET bromodomain family member BRD4 in MPNST. This served as a controlled model system to delineate mechanisms of sensitivity and resistance to BET bromodomain inhibitors in this disease.

Results: Here, we show that a malignant progression–associated increase in BRD4 protein levels corresponds to partial sensitivity to BET inhibition in MPNST. Strikingly, genetic depletion of BRD4 protein levels synergistically sensitized MPNST cells to diverse BET inhibitors in culture and *in vivo*.

Conclusions: Collectively, MPNST sensitivity to combination genetic and pharmacologic inhibition of BRD4 revealed the presence of a unique addiction to BRD4 in MPNST. Our discovery that a synthetic lethality exists between BET inhibition and reduced BRD4 protein levels nominates MPNST for the investigation of emerging therapeutic interventions such as proteolysis-targeting chimeras (PROTACs) that simultaneously target bromodomain activity and BET protein abundance.

Introduction

The discovery of oncogenes, tumor suppressors, and more recently mutational landscapes across human tumors has provided unprecedented knowledge leading to the identification of numerous therapeutic targets against cancer (refs. 1–3; The Cancer Genome Atlas Research Network). Nonetheless, traditional surgery, chemotherapy, and radiotherapy remain as first-line therapeutic strategies for many patients with cancer today (PDQ, National Cancer Institute). However, toxicity of chemotherapy and radiotherapy on normal tissues has spurred interest in the development of cancer tissue–specific therapies (4, 5).

In recent decades, targeted therapy against cancer-specific kinase dependencies has emerged as a promising treatment modality (4–10). However, variable resistance mechanisms have also hindered the therapeutic success of targeted therapies against specific cancer dependencies on kinases such as BCR-ABL, MEK, BRAF, EGFR, and SMO (11, 12). Furthermore, recent awareness of mutational heterogeneity in human tumors through cancer genomic sequencing studies has suggested the need for an expanded arsenal of targeted therapeutics for use either alone or in combination to improve survival of patients with cancer (13, 14).

In contrast, targeted therapy against epigenetic or chromatin regulators has emerged as an attractive alternative strategy against cancer, due, in part, to the fact that these proteins can maintain tumorigenesis through regulation of gene expression programs downstream of both oncogenes and tumor suppressors, and these proteins are druggable (15–20). Epigenetic writers, erasers, and readers are 3 categories of chromatin regulators for which drug targets and small-molecule inhibitors have been developed and shown to be promising targets in either preclinical mouse tumor models or in clinical trials (21–28). Of these, BET bromodomain protein BRD4 has recently emerged as an important chromatin-regulatory protein across multiple cancer types (28–37). BRD4 is critical member of the broader bromodomain and extra-terminal domain (BET) family of epigenetic reader proteins. These include the ubiquitously expressed isoforms BRD4, BRD3, BRD2, and testis-specific isoform BRDT (38). BET proteins are characterized by 2 tandem bromodomains (BDs), which bind acetylated histones to support the recruitment of transcription elongation factor machinery to open chromatin regions, and an extra-terminal domain (ET) that mediates protein–protein interactions (38). Specifically, BET proteins often interact with and

[1]Department of Dermatology, University of Texas Southwestern Medical Center at Dallas, Dallas, Texas. [2]Cancer Biology Graduate Program, University of Texas Southwestern Medical Center at Dallas, Dallas, Texas. [3]Simmons Comprehensive Cancer Center, University of Texas Southwestern Medical Center at Dallas, Dallas, Texas. [4]UTSW Comprehensive Neurofibromatosis Clinic, University of Texas Southwestern Medical Center at Dallas, Dallas, Texas. [5]Hamon Center for Regenerative Science and Medicine, University of Texas Southwestern Medical Center at Dallas, Dallas, Texas.

Note: Supplementary data for this article are available at Clinical Cancer Research Online (http://clincancerres.aacrjournals.org/).

J.M. Cooper and A.J. Patel are the co-first authors of this article.

Z. Chen, C.-P. Liao, and K. Chen contributed equally to this article.

Corresponding Author: Lu Q. Le, Department of Dermatology and Simmons Comprehensive Cancer Center, UT Southwestern Medical Center, 5323 Harry Hines Blvd, Dallas, TX 75390. Phone: 214-648-5781; Fax: 214-648-5553; E-mail: Lu.Le@UTSouthwestern.edu

Clin Cancer Res 2019;25:3404–16

doi: 10.1158/1078-0432.CCR-18-2437

Translational Relevance

Malignant peripheral nerve sheath tumors (MPNSTs) are aggressive sarcomas with no effective therapies. This study reveals a targetable requirement of BRD4 protein level for MPNST survival in the presence of BET inhibitors as genetic depletion of BRD4 synergistically sensitized MPNST cells to diverse BET inhibitors in culture and *in vivo*. This nominates MPNST with high levels of BRD4 for the investigation of emerging therapeutic interventions such as proteolysis-targeting chimeras (PROTACs) that simultaneously target bromodomain activity and BET protein abundance. On the other hand, BRD4-low tumors could be predicted to respond best to strategies using direct BET inhibition alone or in combination with other anticancer agents. These strategies could then be employed in a data-driven manner to provide rational approaches to develop breakthrough treatments for currently therapy-refractory patients with MPNST

support the activity of key transcription factors such as c-MYC, c-Jun, *TP53*, and pTEFb (38, 39). Members of the BET protein family, including BRD4, BRD3, and BRD2 can be potently inhibited pharmacologically with pan-BET bromodomain inhibitors (BET inhibitors) including JQ1, I-BET151, CPI-203, or OTX-015, which competitively bind both bromodomains, perturbing BET protein association with histones and subsequent regulation of gene expression (28–37)

BET inhibitors show great potential as selective, anticancer therapeutics, but the mechanisms underlying sensitivity and resistance to apoptosis in the presence of these inhibitors is less clear. Some recent reports have indicated cancer-specific modes of resistance can occur, such as compensatory kinase signaling in ovarian cancer (40); bromodomain-independent recruitment of BET proteins to chromatin in triple-negative breast cancer (41); and engagement of WNT/β-catenin signaling in acute myeloid leukemia (AML; refs. 42, 43). It has also been reported that BRD4 regulates distinct super-enhancer–associated oncogenes in specific tumor types (e.g., *Myc* in leukemia and multiple myeloma; refs. 44–46). Furthermore, within specific tumor subtypes, there are varying responses to BET inhibitors in preclinical studies and in ongoing phase I clinical trials (47, 48). Although suppression of *Myc* expression has been demonstrated as a mechanism of growth suppression via BET inhibitors, it is not always a key mechanism of action in other tumor types (30, 32, 36, 49). Given these pressing issues, the elucidation of mechanisms governing BET inhibitor sensitivity or resistance would serve as a valuable platform to better understand these inhibitors and develop diagnostic biomarkers for their usage in patients with cancer to maintain the long-term success of this epigenetic therapy.

Recently, we reported that BRD4 plays a critical role in the tumorigenesis of neurofibromatosis type I (NF1)-associated malignant peripheral nerve sheath tumors (MPNST), and that pharmacologic inhibition with BET inhibitor JQ1 is effective in preclinical *in vivo* MPNST tumor studies (34). MPNSTs are highly aggressive sarcomas that develop sporadically or in NF1 patients. There is no effective treatment for MPNSTs and they are typically fatal. We identified a BRD4 dependency in MPNST while studying tumor initiation and progression through step-wise loss of tumor suppressor genes *Nf1* and *Tp53* in neural crest–related skin-derived precursor cells (SKP), which we recently established as an *ex vivo* transplantable model of MPNST development (34, 50, 51). Thus, we reasoned that this model would serve as a controlled system to delineate genetic mechanisms of sensitivity or resistance to JQ1 in MPNST.

Shortly after our study was published, 3 independent groups reported that loss of function in members of the polycomb repressor complex 2 (PRC2) is a characteristic of MPNST (23, 52) and even promotes sensitivity to BET inhibition (53). PRC2 loss of function results in reduced H3K27 methylation and allows for subsequent H3K27 acetylation, which mediates BRD4 recruitment to chromatin. These studies suggest that, in MPNST, PRC2 loss of function allows for histone priming for BRD4 recruitment and activation, facilitating its role in maintaining MPNST survival and nominating its use as a therapeutic target. Importantly, these observations illustrate how BRD4 dependency is possible even in the absence of mutations in BRD4 interactor *TP53*, as *TP53* mutations and loss-of-function mutations in PRC2 members are often nonredundant in MPNST patient tumor samples (54). However, PRC2 loss of function may not confer sensitivity to BET inhibition in all cancer contexts, as it can actually promote BET inhibitor resistance in AML (42). Importantly, however, we also observed in MPNST that BRD4 inhibition with JQ1 or RNAi promotes active engagement of apoptosis through upregulation of proapoptotic Bim and downregulation of antiapoptotic Bcl2 (34). This is consistent with the observation that the preclinical antitumor efficacy of BET inhibition is, in part, dependent on the degree to which their administration engages apoptosis (55). It was in light of these observations that we chose to explore modes of BET inhibition sensitivity and resistance in MPNST and in so doing uncovered a targetable BRD4 protein addiction in this disease.

Materials and Methods

Cells and reagents

Primary mouse MPNST (mMPNST) cells were generated via a mouse MPNST model as described previously (34, 50, 51). Human S462 MPNST cells were a kind gift from Karen Cichowski (Harvard Medical School, Boston, MA). Human MPNST cells were authenticated with human-specific PCR primers on September 18, 2018 to confirm the absence of mouse tumor cell contamination. All leukemia cell lines were a kind gift from Dr. Chengcheng Zhang [UT Southwestern (UTSW), Dallas, TX]. Routine *Mycoplasma* testing of the cell lines was not performed. All cells were cultured in DMEM (10% FBS, 1% L-glutamine, 1% sodium pyruvate, 1% penicillin–streptomycin). Drugs used: JQ1 (Cayman Chemical and MedChem Express), OTX-015 (Cayman Chemical), CPI-203 (Cayman Chemical), CPI-0610 (Axon Medchem), ARV-771, and ARV-825 (MedChem Express).

Animal studies

All mice were housed in the animal facility at the University of Texas Southwestern Medical Center at Dallas (Dallas, TX). Animal care and use were approved by the Institutional Animal Care and Use Committee (IACUC) at UTSW (Dallas, TX). Female athymic nude mice ($\geq$ 8 weeks old) obtained from The Jackson Laboratory were used for tumor studies. *In vivo* induction of shRNAs in mMPNST-pTripz tumors, JQ1 dosing, and tumor bioluminescence imaging were all carried out as described previously (34).

In vivo administration of ARV771 BET proteolysis-targeting chimera (PROTAC) was conducted using a modified treatment regimen from refs. 56–58. Briefly, tumorigenic clones of S462 were subcutaneously injected into the right and left hind flank of 10 mice per treatment group (2×10^6 cells per tumor). Xenograft tumors were allowed to form until palpable (2 weeks). Tumors were measured by electronic caliper on treatment experiment day 0 (Volume = $L \times W^2 \times 0.5$), and mice were divided between treatment groups ($n = 10$ mice) so that the average tumor size per group reach approximately 45 mm^3. Vehicle (5% Sorbitol HS15 and 5% EtOH in D5W) or 30 mg/kg ARV771 were subcutaneously injected daily (beginning on experiment day 1) for the length of treatment period. Mouse weight changes (to evaluate treatment toxicity) and tumor volume measurements were routinely collected throughout the treatment period. As in refs. 56–58, all mice received a drug holiday of 1–2 days during the course of the treatment. On day 20 of the treatment period (1 day after the final dose), final measurements of tumor volume and tumor mass were conducted.

Brd4 Knockout by CRISPR/Cas9 genomic editing

Doxycycline-inducible Cas9 cDNA lentiviral vector (Addgene plasmid #50061 = pCW-Cas9) and additional lentivector constitutively expressing AAVS1-targeting sgRNA (sgCON; Addgene plasmid #50662 = pLX-sgRNA) or sgBRD4.1 lentivector (pLX-sgRNA vector with AAVS1-sgRNA+PAM_sequence replaced with the following *Brd4*-targeting sgRNA+PAM_sequence: GTTCAGCTTGACGGCATCCA) were packaged into lentiviral particles that were used to infect, and select for transduced cells. *Brd4* sgRNA was designed using E-CRISP software (http://www.e-crisp.org/E-CRISP). For genomic editing, stably infected cells were plated as single-cell clones, followed by Cas9 induction for 10 days with doxycycline. Single-cell clone outgrowths were expanded, and screened as described previously (59, 60). To determine the efficacy of CRISPR/Cas9 gene editing, genomic DNA was extracted from mouse MPNST cells (parental, sgCON clones 1 and 2, and sgBRD4.1 clones 3, 4, and 13) and the genomic region surrounding the *Brd4* sgRNA-targeted sequence was amplified by PCR [primers used: 5′–3′ (F3: CTAACAAGCCCAAGAGACAG, R3: CCAACTTTACCCTTCTGCAG)]. The amplified PCR product was submitted for Sanger sequencing by the McDermott Center Sequencing Core Facility at UTSW (Dallas, TX). The PCR products of sgBRD4.1_Clone 4 and sgBRD4.1_Clone 13 were further subcloned into pGEM-T Easy (Promega) cloning plasmids for additional Sanger sequencing via T7 primers. Sequence similarity was assessed using the Basic Local Alignment Search Tool (BLAST) provided by the NCBI.

Lentiviral constructs

Mouse/human *Brd4* shRNAs were generated as described previously (34). Human *Brd3* shRNAs were generated by cloning of the following 21-mer sequences (shBrd3.a: CCAAGGAAATGTCTCGGATAT, shBrd3.b: GCTGATGTTCTCGAATTGCTA, shBrd3.c: CCCAAGAGGAAGTTGAATTAT) into the pLKO.1-puro empty backbone lentiviral vector.

In vitro growth measurements

ATP CellTiter Glo assay (Promega) was carried out according to modified manufacturer's recommendations. Luminescence was quantified via Synergy|HT 96-well plate reader (BioTek).

Quantification of cellular apoptosis

For analysis of cellular apoptosis/death, FITC-AnnexinV Kit (Miltenyi Biotec) or APC-AnnexinV Kit (BioLegend) was used as per modified manufacturer's instructions. The FACSCalibur, FACSCanto, and FACSLyric Flow Cytometers (BD Biosciences) at the UTSW Flow Cytometry Core Facility and the Moody Foundation Flow Cytometry Facility of the Children's Research Institute (CRI) at UTSW (Dallas, TX) were used for cellular analyses. Cytobank and FlowJo software (Tree Star) were utilized for data visualization and analyses.

RNA isolation, cDNA synthesis, and qRT-PCR

All procedures were performed as described in ref. 34. Data were quantified by ΔC_t method and normalized relative to *Gapdh* (housekeeping gene). The following primers were used (5′–3′): hBrd4_F, AGTTTGCATGGCCTTTCC; hBrd4_R, CCTGAGCATTCCAGTAATAGTTG; hBrd3_F, GAAGGCCAACAGCACGAC; hBrd3_R, CCCTCCTCCTCTTCCTCTGA.

Western blot analysis

Western blot procedures were carried out as described previously (51, 61). The following antibodies were used: BRD4 (Bethyl Laboratories); GAPDH, BRD3, BRD2 (Santa Cruz Biotechnology), α/β-Tubulin (α,β-Tubulin), Bim, cleaved caspase-3, cleaved PARP, and Histone 3 (Cell Signaling Technology).

Statistical analyses

Data are displayed as the mean ± SEM. Two-tailed unpaired Student *t* test was used to evaluate statistical significance ($P < 0.05$ was deemed statistically significant).

Results

BRD4 levels underlie resistance to BET inhibitor–induced death in MPNST cells

Previously, we observed that malignant progression of normal SKPs to MPNST via inactivation of both *Nf1* and *Tp53* was associated with increased levels of BRD4 (34). Interestingly, it has been reported that increased levels of BRD4 are associated with increased sensitivity to BET inhibitor JQ1 in the context of Notch1 inhibitor–resistant T-cell leukemia (62). As MPNST cells expressing elevated BRD4 exhibit enhanced sensitivity to JQ1 over pretumorigenic, BRD4-low SKPs (34), we hypothesized that increased levels of BRD4 confer JQ1 sensitivity in this context. We suspected that JQ1 resistance would arise from MPNST cells with lower BRD4 levels that are insensitive to JQ1 inhibition. Thus, we reasoned that stable suppression of BRD4 expression would desensitize BRD4-high MPNSTs to JQ1. Through CRISPR/Cas9-based genome editing (Fig. 1A; Supplementary Fig. S1A–S1F) and the heterogeneity of endogenous BRD4 expression levels in MPNST cells, we generated *Brd4*-depleted mouse MPNST (mMPNST) cell clones that offer different levels of BRD4 expression for us to model JQ1 sensitivity as a function of BRD4 levels through functional assays (Fig. 1B). We employed targeted sequencing of representative sgControl and sg*Brd4* clones to determine the exact mutations in each of the sg*Brd4*-targeted lines. As expected, parental mMPNST cells and both sgControl clones (c1 and c2) have no *Brd4* mutation (Supplementary Fig. S1A–S1C). sg*Brd4* clone c3 also has no *Brd4* mutation (Supplementary Fig. S1D); and accordingly maintains BRD4 protein expression (Fig. 1B). Most importantly, we found that a single

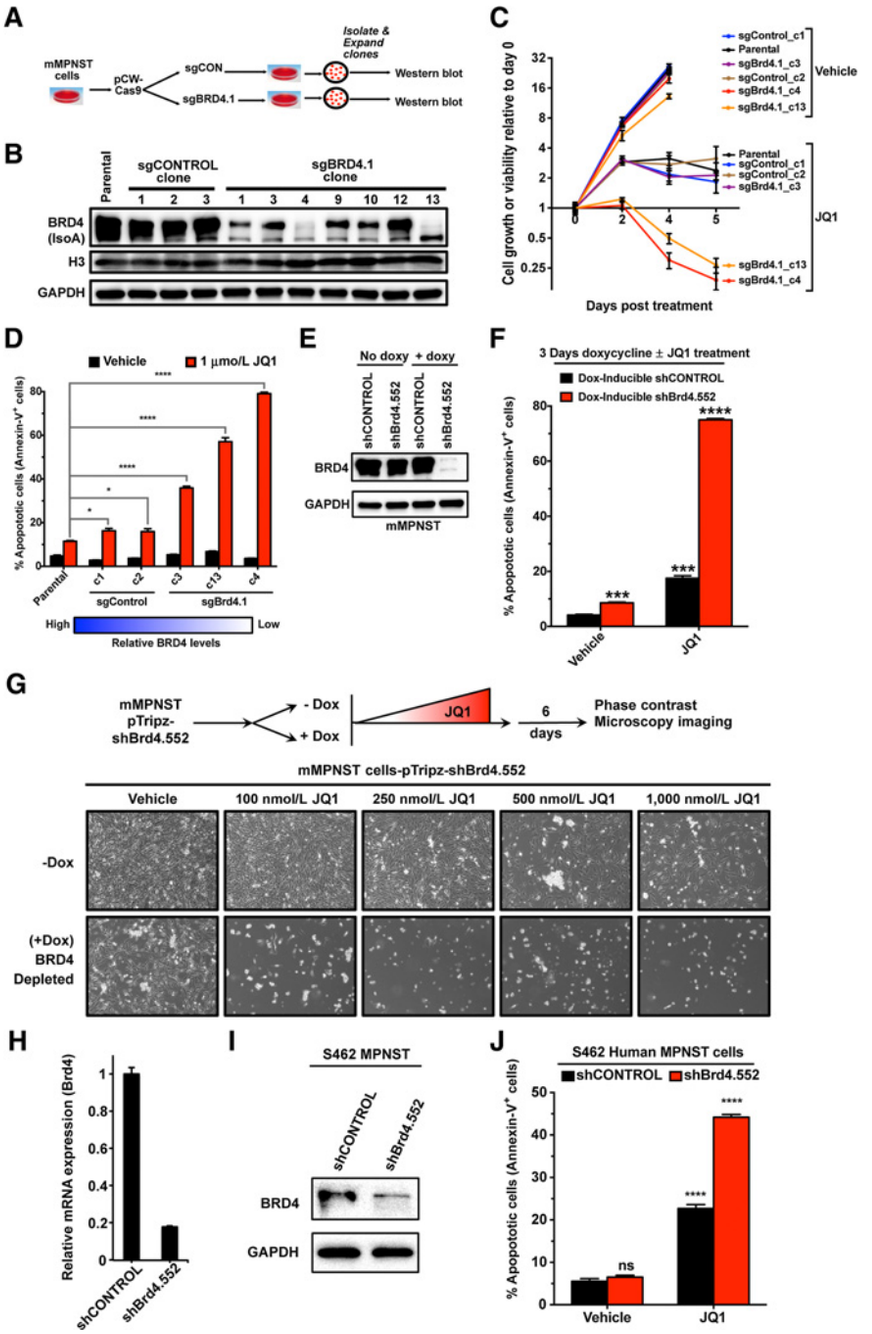

Figure 1.

BRD4 depletion overcomes resistance to BET inhibitor–induced cell death in MPNST **A,** Diagram illustrating the generation of mouse MPNST cells (mMPNST) with *Brd4* knockout via CRISPR-Cas9–based genomic editing. **B,** Western blot analysis of BRD4 protein expression in mMPNST cell clones isolated after induction of CRISPR-Cas9 genomic editing with sgRNAs (sgCONTROL or sgBRD4.1) relative to parental mMPNST cells. **C,** mMPNST cells with or without *Brd4* knockout were treated with vehicle or 1 μmol/L JQ1 followed by cell viability analysis via ATP CellTiter-Glo assay at the indicated time points. **D,** mMPNST cells with or without *Brd4* knockout were treated with vehicle or 1 μmol/L JQ1 for 4 days followed by flow cytometry analysis for Annexin V (+) apoptotic cells. **E,** Western blot validation of doxycycline (Dox)-inducible shRNA-mediated knockdown of BRD4 in mMPNST cells (3 days after doxycycline treatment). **F,** mMPNST cells were treated with doxycycline (to induce shCONTROL or shBrd4.552) in tandem with vehicle or 1 μmol/L JQ1 for 3 days followed by flow cytometry analysis for Annexin V (+) apoptotic cells. **G,** mMPNST cells were treated with or without doxycycline (to induce shBrd4.552) in tandem with vehicle or JQ1 at the indicated doses followed by cell viability analysis via phase contrast microscopy after 6 days. **H,** Validation of *BRD4* knockdown in human S462 MPNST cells by qRT-PCR. **I,** Western blot validation of constitutive BRD4 protein knockdown in S462 MPNST cells with shRNAs as listed. **J,** S462 MPNST cells with or without constitutive BRD4 knockdown were treated with vehicle or 1 μmol/L JQ1 for 4 days followed by flow cytometry analysis for Annexin V (+) apoptotic cells. All error bars and statistics are represented as the mean ± SEM (*, $P \leq 0.05$; **, $P \leq 0.01$; ***, $P \leq 0.001$; ****, $P \leq 0.0001$).

base pair (bp) insertion in one allele and a 50-bp deletion in the other allele in the sg*Brd4*-targeted clone c4 (Supplementary Fig. S1E), as well as a 2-bp insertion in one allele and a 13-bp deletion in the other allele in the *sgBrd4*-targeted clone c13 (Supplementary Fig. S1F), each resulted in loss of BRD4 protein expression (Fig. 1B). When these cells along with control cells were monitored for growth and apoptosis after JQ1 treatment, we observed hypersensitivity to JQ1 in *Brd4*-knockout MPNST cells (Fig. 1C and D; Supplementary Fig. S2A), which was unexpected given our initial hypothesis. Interestingly, MPNST cells maintaining BRD4 expression (e.g., c1, c2, c3), showed intermediate levels of cell death with JQ1, while cells with BRD4 knockout (e.g., c4) displayed near-maximal cell death (Fig. 1D). Together, these findings led us to refine our model in which we suggest that the persistence of higher BRD4 levels posttreatment can mediate resistance in BET inhibitor–treated MPNST cells.

BRD4 depletion overcomes resistance to BET inhibitor–induced cell death in MPNST

To exclude the possibility that these results were due to the selection of single-cell clones with preexisting sensitivities to JQ1, we utilized potent doxycycline-inducible shRNA against *Brd4*. Upon doxycycline addition, we observed almost complete loss of BRD4 protein levels (similar to a knockout; Fig. 1E) compared

with scrambled control (shCONTROL). These phenotypes were verified with multiple shRNAs in our previous studies (34). We utilized this sensitive yet rapid system to acutely knockdown *Brd4* and monitor survival of MPNST cells with or without JQ1 treatment (Fig. 1F). We observed massive cell death (70%–80% apoptosis) in as few as 3 days when doxycycline-induced *Brd4* knockdown was combined with JQ1, while cell death occurred to a far lesser extent in controls as expected (Fig. 1F). Using this system, we observed that low doses of JQ1 were also sufficient to cooperate with acute *Brd4* depletion to kill most MPNST cells in culture by 6 days, while control cells remained largely viable, but growth inhibited as expected (Fig. 1G; Supplementary Fig. S2B). We have previously shown that apoptotic cell death induced upon BRD4 inhibition by shRNA or small-molecule BET inhibitors in MPNST cells occurs through upregulation of proapoptotic signaling protein Bim and downregulation of antiapoptotic proteins such as Bcl-2 (34). Consistent with our previous findings, apoptotic induction upon JQ1 treatment was enhanced when MPNST cells were cotreated with JQ1 and Bcl-2 inhibitor ABT263 (Supplementary Fig. S2C). Cotreatment with JQ1 and ABT263 also abrogated cellular proliferation more than either inhibitor alone (Supplementary Figs. S2D and S2E). Bcl-2 inhibition exhibited a smaller additive effect on apoptosis and cell proliferation in sh*Brd4* cells treated with JQ1 than in JQ1-treated shControl cells, indicative that JQ1 treatment in the context of BRD4 depletion already approached maximal apoptosis engagement and cell proliferation inhibition (Supplementary Figs. S2C–S2E).

Given that BET inhibitors (e.g., JQ1) can inhibit multiple BET proteins in humans, we investigated whether the depletion of BET bromodomain proteins in human MPNST cells would phenocopy what we observed in mouse mMPNST cells. Consistent with our data thus far, we observed that shRNA-mediated constitutive depletion of BRD4 (Fig. 1H and I) conferred extreme sensitivity to JQ1-induced cell death compared with JQ1-treated shControl cells (Fig. 1J). Similarly, we found that knockdown of BET family member *BRD3* was slightly growth inhibitory and toxic to MPNST cells, but it conferred acute sensitivity to JQ1 cotreatment (Supplementary Fig. S3A and S3C), although to a smaller extent than *BRD4* knockdown. These data reveal that both BRD3 and BRD4 can support MPNST cell growth and that depletion of either one of them can sensitize human MPNST cells to BET inhibitor–induced death, suggesting BET bromodomain family members may possibly play coordinate roles in maintaining MPNST cell growth and survival. Because persistent genetic deletion of BRD4 did not markedly alter the protein levels of BRD3 or BRD2 (Supplementary Fig. S2A), it is likely any coordinate roles in this system would occur at the level of BRD4/3/2 function, rather than expression.

Genetic inhibition of BRD4 overcomes MPNST cell resistance to diverse BET inhibitors

Having found that genetic depletion or knockout of *Brd4* rendered extreme sensitivity to BET inhibitor JQ1 in MPNST cells, we expanded our investigation to include alternative BET inhibitors. To exclude the possibility that our observations were biased by the polypharmacology of JQ1, we additionally utilized OTX-015, CPI-203, and CPI-0610, which are broad-spectrum BET inhibitors previously shown to inhibit BRD2, BRD3, and BRD4 (63–65). Comparative dose–response analysis of JQ1, OTX-015, and CPI-203 revealed similar growth-inhibitory effects of these 3 independent BET inhibitors on both mouse and human MPNST cells (Fig. 2A and B). Upon cell death analysis (Fig. 2C), a 1 μmol/L dose consistently led to about 15% cell death with each inhibitor, and higher doses (up to 20 μmol/L) of either JQ1 or OTX-015 led to further enhanced cell death in a dose-dependent manner. In contrast, MPNST cells were relatively resistant to higher doses of CPI-203 (Fig. 2C). Remarkably, when MPNST cells were BRD4-depleted, cotreatment with a 1 μmol/L dose of CPI-203 led to massive cell death that was comparable with the same dose of JQ1 or OTX-015 (Fig. 2D). CPI-0610 displayed similar, although less potent, inhibition of MPNST cell viability as JQ1 in shCONTROL cells; however, depletion of *Brd4* was sufficient to sensitize MPNST cells to BET inhibition by CPI-0610, particularly as the dose was increased (Fig. 2E and F). These comparative analyses reveal that genetic inhibition of BRD4 can overcome MPNST resistance to a spectrum of BET inhibitors with differing intrinsic potencies.

BRD4-high MPNST cells are sensitive to titrated BRD4 depletion by PROTACs

Our studies to this point suggest that BRD4-addicted tumors would likely harbor resistance to BET inhibition alone, but could be sensitized by targeted depletion of BRD4. While this is relatively straightforward *in vitro*, genetic depletion of *BRD4* by RNAi or CRISPR in humans is fraught with challenges making it not presently therapeutically viable. Recent developments in chemical biology have sought to address the problem of achieving depletion of specific proteins in cells and *in vivo* without the use of oligonucleotides through the development of PROTACs (66). PROTACs contain a binding moiety against a target of interest, a linker region, and a separate binding moiety for an E3 ubiquitin ligase. The linker region allows for the specific localized ubiquitination of the target protein of interest for degradation by the E3 ligase that has been brought into its unique proximity by the PROTAC. To assess whether selective degradation of BRD4 is achievable in the context of MPNST, we employed 2 PROTAC molecules, ARV825, which employs a Cereblon E3 ligase–mediated degradation of BRD4 (67), and ARV771, which utilizes the von Hippel-Lindau (VHL) E3 ligase to degrade BRD4 (56). In human MPNST cells, both PROTACs elicited dose-dependent, persistent degradation of BRD4 following 3 days of treatment (Fig. 3A). ARV771 was slightly more potent in this context than ARV825, as 1 μmol/L (the most effective dose of either PROTAC) ARV771 produced near undetectable levels of BRD4, while 1 μmol/L of ARV825 allowed for noticeable residual BRD4 expression (Fig. 3A). The degradation of BRD4 corresponded to dose-dependent upregulation of cell death markers cleaved PARP and cleaved caspase-3, and also induced apoptotic cell death (Figs. 3A and B). In addition, both PROTAC molecules displayed a near 10-fold reduction of IC_{50} for cell viability compared with JQ1 (Fig. 3C) in human MPNST cells.

While ARV825 and ARV771 were originally designed to target human BRD4, we also confirmed that they exhibit dose-dependent depletion of BRD4 and engagement of apoptosis in mouse mMPNST cells (Fig. 3D and E). In mMPNST cells, ARV825 was more potent than ARV771 in inducing apoptosis, particularly at 1 μmol/L, which corresponded to greater BRD4 depletion by ARV825 at the same doses (Fig. 3D and E). In addition, in mMPNST cells, both PROTACs inhibited cell viability more potently than JQ1 at their highest dose (Fig. 3F). In both mouse and human cells, we observed that the levels of BRD4 began to rise between 1 μmol/L and 10 μmol/L doses (Fig. 3A and D). This is

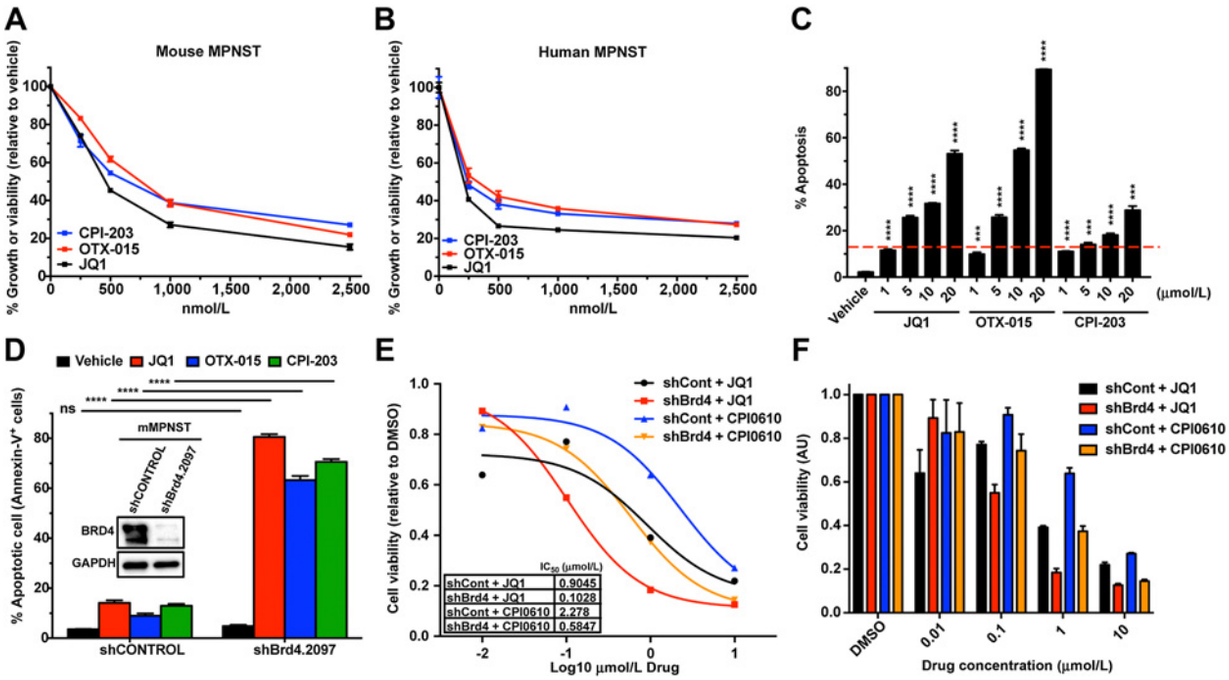

Figure 2.

Genetic inhibition of BRD4 overcomes MPNST cell resistance to diverse BET inhibitors. mMPNST (**A**) and S462 MPNST (**B**) cells were treated with BET inhibitors CPI-203, JQ1, or OTX-015 at the indicated concentrations for 3 days followed by cell viability analysis via ATP CellTiter-Glo assay. **C,** mMPNST cells were treated with vehicle or BET inhibitors CPI-203, JQ1, or OTX 015 at the indicated concentrations for 4 days, followed by flow cytometry for Annexin V (+) apoptotic cells. **D,** mMPNST cells with or without *Brd4* depletion were treated with vehicle or 1 μmol/L of the indicated BET inhibitors followed by flow cytometry for Annexin V (+) apoptotic cells after 4 days (Inset: Western blot validation of shRNA mediated *Brd4* depletion in mMPNST cells). **E** and **F,** Comparative analysis of pan-BET inhibitors JQ1 and CPI-0610 on mMPNST cell viability. shControl and sh*Brd4* cells were treated with doxycycline and JQ1 or CPI-0610 for 3 days followed by ATP CellTiter-Glo assay. Data are plotted as multipoint dose–response curves relative to vehicle (DMSO; **E**) and as individual treatment points relative to vehicle (DMSO; **F**). All error bars and statistics are represented as the mean ± SEM (*, $P \leq 0.05$; **, $P \leq 0.01$; ***, $P \leq 0.001$; ****, $P \leq 0.0001$).

likely an example of a "hook effect" that has been observed for PROTACs, as increasing compound concentrations begin to out-compete themselves for binding to the target of interest, which results in reduced target degradation (68). Cotreatment of the PROTACs (1 μmol/L) with JQ1 (1 μmol/L) produced little to no additional induction of apoptosis compared with either PROTAC alone (Fig. 3B and E), indicating that at this dose PROTAC treatment has maximally engaged the apoptotic response possible for BRD4 inhibition. In addition, cotreatment of JQ1 with either PROTAC molecule produced less BRD4 protein depletion than PROTAC treatment alone (Fig. 3A and D). Because the BRD4-binding moiety in the PROTAC targets the same binding site on BRD4 as JQ1, this blunting of BRD4 depletion suggests that the addition of JQ1 may have lowered the effective concentration of the PROTAC, as it competed with PROTAC for binding to BRD4. Together, these results are proof-of-principle experiments that show a PROTAC-mediated strategy for both BRD4 depletion and BET inhibition may be a viable avenue to target BRD4-addicted MPNSTs in human patients via a single-cell–permeable small molecule.

PROTAC-mediated BRD4 depletion can bypass BRD4-high leukemia cell resistance to BET inhibitors

Given previous reports that BET bromodomain family members such as BRD4 support the growth and proliferation of hematopoietic cancers such as AML and CML, we sought to validate whether the synthetic lethality we observed between BRD4 depletion and BET pharmacologic inhibition applied to broader cancer contexts beyond MPNST. We focused on a panel of human leukemia cells that possessed distinct oncogenic mutations and had been previously found to have differential sensitivities to JQ1 (31, 36). Baseline analysis of BRD4 expression in the 4 leukemia lines examined revealed that K-562 (CML) and Kasumi-1 (AML) displayed relatively higher levels of BRD4, while both HL-60 (AML) and THP-1 (AML) showed relatively lower levels of BRD4 (Fig. 4A). Importantly, K-562 cells, which displayed the highest levels of baseline BRD4, are known to harbor resistance to BET inhibitors (31, 36). These cells displayed no noticeable apoptotic induction and limited perturbation of cell viability when treated with JQ1, compared with the other cell lines tested (Fig. 4B and C). Strikingly, both HL-60 and THP-1 cells, which both exhibited relatively lower levels of BRD4, were extremely sensitive to apoptosis induction upon JQ1 treatment (Fig. 4B). Interestingly, we found that these differences among the leukemia cell lines extended to a cell viability assay in which lower-expressing BRD4 cells (HL-60 and THP-1) were most potently sensitive to JQ1 in a dose-dependent manner (Fig. 4C). We then examined whether leukemia cell lines expressing higher levels of BRD4 would be more sensitive to BRD4 inhibition by PROTAC than to BET-bromodomain antagonists. Similar to our

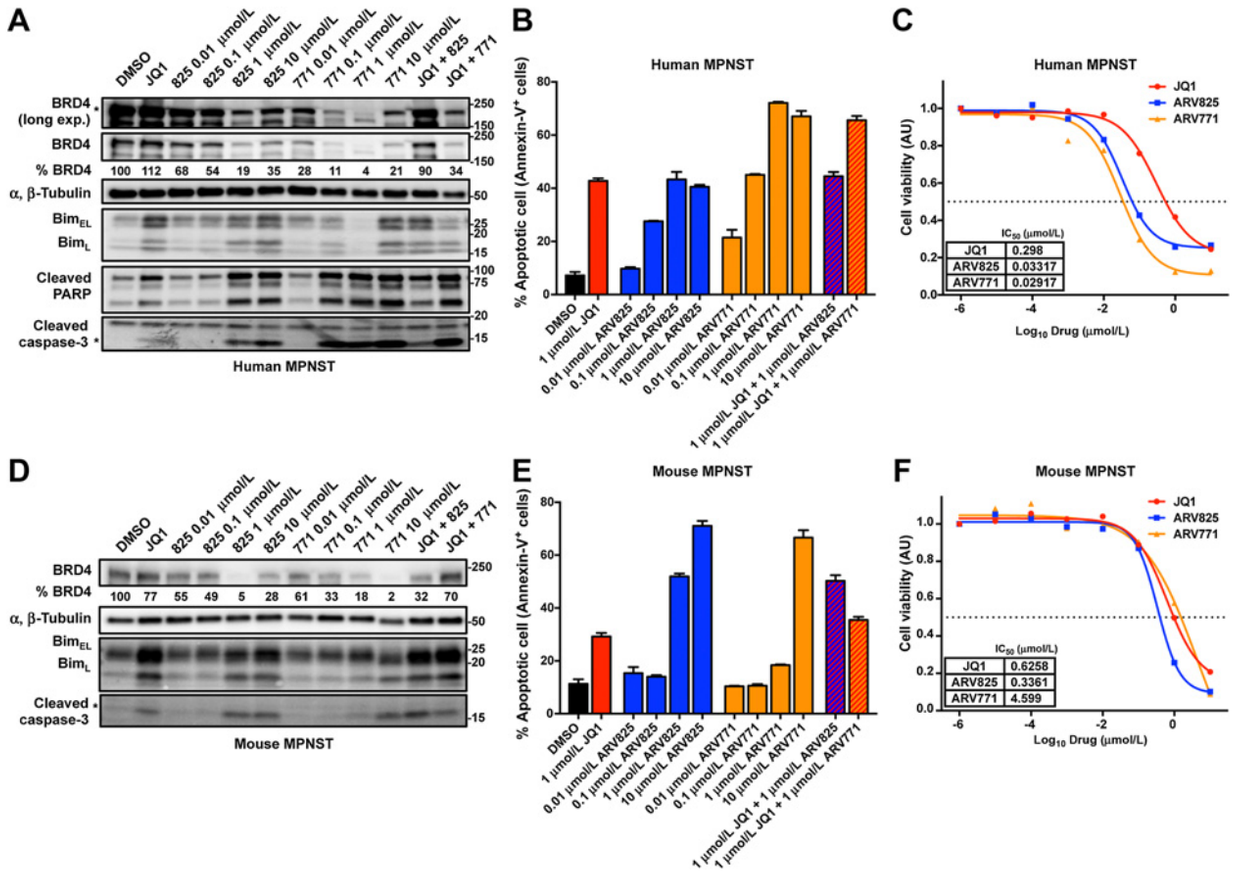

Figure 3.

BRD4-high MPNST cells are sensitive to titrated BRD4 depletion by PROTACs. **A** and **B,** Anti-BRD4 PROTACs produce dose-dependent depletion of BRD4 and induction of apoptosis in human S462 MPNST cells. **A,** Western blot analysis of BRD4 and apoptosis induction markers following 3-day treatment with DMSO, 1 μmol/L JQ1, ARV825 (825), ARV771 (771), 1 μmol/L JQ1 + 1 μmol/L 825, or 1 μmol/L JQ1 + 1 μmol/L 771. Densitometry percentages for BRD4 (BRD4/α,β-tubulin) were calculated via ImageJ and are listed relative to DMSO. **B,** S462 MPNST cell death induction under the same treatment concentrations as **A** for 3 days, followed by flow cytometry for Annexin V (+) apoptotic cells ($n = 3$ per treatment). **C,** Comparative analysis of JQ1, ARV825, and ARV771 on human S462 MPNST cell viability. shControl S462 cells were treated with compounds as listed for 3 days followed by ATP CellTiter-Glo assay. Data are plotted as multipoint dose–response curves ($n = 3$ per treatment) normalized to the lowest treated dose (1 pmol/L). **D** and **E,** Anti-BRD4 PROTACs produce dose-dependent depletion of BRD4 and induction of apoptosis in mMPNST cells. **D,** Western blot analysis of BRD4 and apoptosis induction markers following 3-day treatment as in **A**. Densitometry percentages for BRD4 (BRD4/α,β-tubulin) were calculated via ImageJ and are listed relative to DMSO. **E,** mMPNST cell death induction under the same treatment concentrations as **D** for 3 days, followed by flow cytometry for Annexin V (+) apoptotic cells ($n = 3$ per treatment). **F,** Comparative analysis of JQ1, ARV825, and ARV771 on mMPNST cell viability. shControl mMPNST cells (no doxycyline) were treated with compounds as listed for 3 days followed by ATP CellTiter-Glo assay. Data are plotted as multipoint dose–response curves ($n = 3$ per treatment) normalized to the lowest treated dose (1 pmol/L). All error bars are represented as the mean ± SEM.

observations in MPNST, 3-day treatment of K-562 or Kasumi-1 cells with ARV771 potently mediated BRD4 depletion to nearly undetectable levels, and this corresponded to a marked induction of apoptotic cell death compared with BET inhibitors JQ1, OTX015, and CPI-0610 (Fig. 4D and E). Interestingly, treatment of Kasumi-1 cells with each of the 3 BET inhibitors, but not the PROTAC, corresponded to an increase of BRD4 levels after treatment, compared with vehicle control (Fig. 4E). As BRD4 upregulation in response to BET bromodomain antagonists has been reported previously (67) and may serve as a mechanism of resistance, we inquired whether BET inhibitors were less able to inhibit Kasumi-1 cell viability than a BET PROTAC, which suppressed BRD4 levels over the course of treatment. PROTAC treatment displayed a greater than 100-fold decrease in IC_{50} compared with all 3 BET inhibitors assayed for effects on cell viability in BRD4-high Kasumi-1 cells (Fig. 4F). Interestingly, combination administration of JQ1 and ARV771 in K-562, Kasumi-1 and human MPNST cells displayed little to no added effect above single-agent treatment alone, with ARV771-mediated apoptosis induction being the consistently dominant phenotype (Fig. 3B; Supplementary Fig. S4A–S4D), even at doses below 1 μmol/L. This is likely explained by the fact that both JQ1 and ARV771 are compensative inhibitors of the same sites on BRD4 and the other BET proteins (56), and thus would likely compete with each other for target binding if combined, as mentioned above. These data suggest that BRD4-high cancer cells that display relative resistance to small-molecule BET inhibitors retain a vulnerability to targeted degradation of BRD4 proteins by a PROTAC therapeutic strategy.

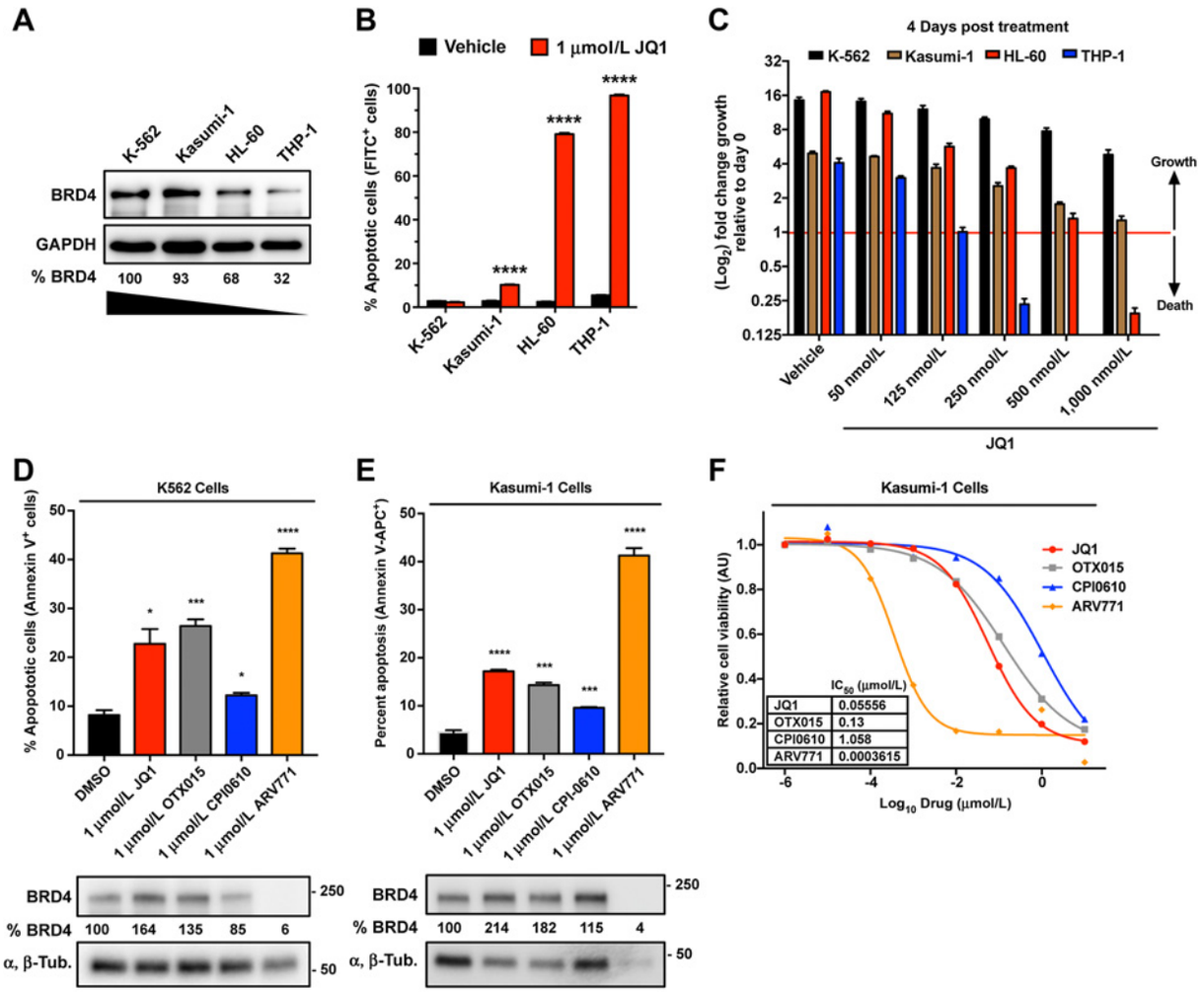

Figure 4.

PROTAC-mediated BRD4 depletion can bypass BRD4-high leukemia cell resistance to BET inhibitors. **A,** Western blot analysis of relative baseline BRD4 protein expression in leukemia cell lines. Densitometry percentages for BRD4 (BRD4/GAPDH) were calculated via ImageJ and are listed relative to K-562 cells. **B,** Leukemia cell lines were treated with vehicle or 1 μmol/L JQ1 for 4 days followed by flow cytometry analysis for Annexin V (+) apoptotic cells. **C,** Leukemia cell lines were treated with vehicle or JQ1 at the indicated concentrations for 4 days followed by cell viability analysis via ATP CellTiter-Glo assay. **D** and **E,** Effect of PROTAC-mediated BRD4 depletion versus BET inhibitor treatment on apoptosis induction in K-562 (**D**) or Kasumi-1 (**E**) leukemia cells, as assessed by flow cytometry for Annexin V (+) cells ($n = 3$ per treatment) and by Western blotting for BRD4 expression (3 days after treatment). Densitometry percentages for BRD4 (BRD4/α,β-Tubulin) were calculated via ImageJ and are listed relative to vehicle (DMSO). **F,** Comparative analysis of BET inhibitor or PROTAC treatment on Kasumi-1 cell viability. shControl Kasumi-1 cells were treated with compounds as listed for 3 days followed by ATP CellTiter-Glo assay. Data are plotted as multipoint dose–response curves ($n = 3$ per concentration) normalized to the lowest treated dose (1 pmol/L). All error bars and statistics are represented as the mean ± SEM (*, $P \leq 0.05$; **, $P \leq 0.01$; ***, $P \leq 0.001$; ****, $P \leq 0.0001$).

Genetic inhibition of BRD4 improves BET inhibitor therapeutic efficacy against MPNST tumors *in vivo*

We next investigated whether suppression of BRD4 expression in BRD4-high/addicted MPNST tumors could improve or enhance the therapeutic efficacy of BET inhibition *in vivo*. Toward this end, we utilized *Nf1/Tp53*-inactivated mMPNST cells (luciferase-expressing) that possess both high baseline levels of BRD4 and doxycycline (Dox)-inducible shRNAs (shCONTROL or sh*Brd4*). We implanted these tumor cells in nude mice and allowed solid tumors (<100 mm^3) to form. This was followed by activation of sh*Brd4* or shCONTROL with doxycycline in all tumors in combination with daily vehicle or JQ1 administration to the mice for 20 days (Fig. 5A). Through measurement of palpable tumor volume and *in vivo* bioluminescence imaging at multiple points during this experiment, we observed a remarkable and significant therapeutic improvement when *Brd4* knockdown was combined with JQ1 (Fig. 5B–F), whereas *Brd4* knockdown or JQ1 treatment alone showed far lesser efficacy. During this treatment period, we also observed that, consistent with our previous results, JQ1-treated tumors underwent maximal tumor regression after 5 days followed by a rapid relapse of these tumors at a slower growth rate compared with vehicle-

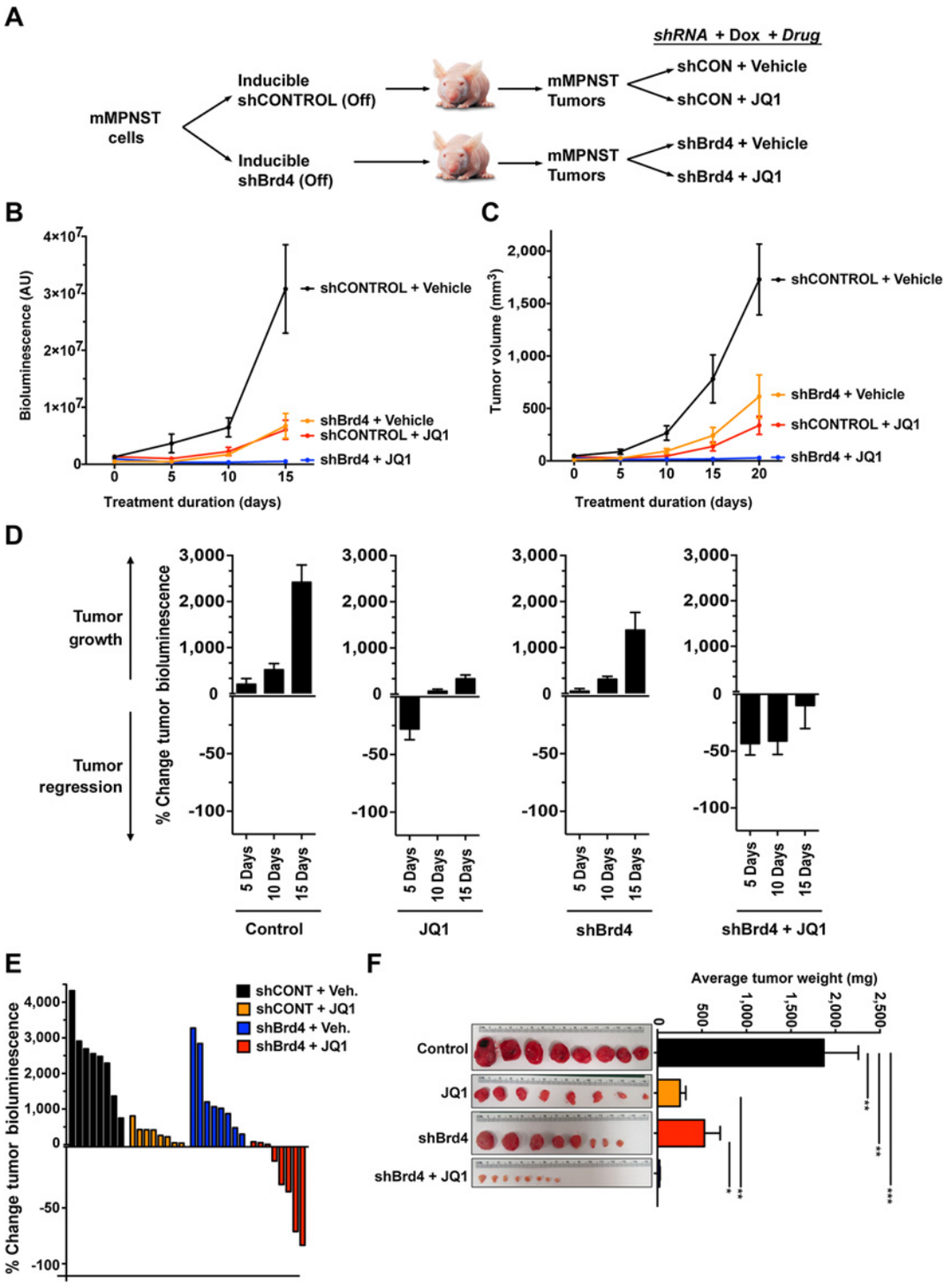

Figure 5.

Genetic inhibition of BRD4 improves BET inhibitor therapeutic efficacy against MPNST tumors *in vivo*. **A,** Flowchart diagram illustrating experimental outline for genetic and pharmacologic inhibition of BRD4 in mMPNST allograft tumors *in vivo*. **B,** Tumor growth curves of raw bioluminescence values from luciferase-expressing mMPNST allograft tumors *in vivo*. **C,** Tumor growth curves of mMPNST allograft tumor volume (mm^3). **D,** Tumor growth or regression assessed by percent change in bioluminescence of luciferase-expressing mMPNST allograft tumors. **E,** Waterfall plot of final percent change (at 15 days posttreatment) in bioluminescence of each luciferase-expressing mMPNST allograft tumor per treatment group. **F,** Photographs of mMPNST tumors isolated from mice treated with the indicated treatment regimen for 20 days (left), and average final weight of tumors from each treatment group (right). All error bars and statistics are represented as the mean ± SEM (*, $P \leq 0.05$; **, $P \leq 0.01$; ***, $P \leq 0.001$; ****, $P \leq 0.0001$).

treated tumors (Fig. 5D). In contrast, tumors with *Brd4* knockdown plus JQ1 treatment had more striking tumor regression within the first 5 days followed by a suppression of tumor relapse (Fig. 5D). Even at 15 days posttreatment, over half of the tumors in the JQ1 plus sh*Brd4* group exhibited greater than 30% tumor regression (Fig. 5E). Analysis of final tumor weight after 20 days of treatment was consistent with these observations (Fig. 5F). These data collectively point to an *in vivo* synthetic lethality between *Brd4* depletion and BET inhibitor treatment in MPNST.

As RNAi-mediated targeting of BRD4 in human patients is not a presently viable therapeutic modality, we examined whether single-agent BET PROTAC treatment could translate our murine MPNST model results into a human MPNST xenograft model for the treatment of human MPNSTs. We established an S462 xenograft–derived cell line (S462-021L), which possessed heightened tumorigenic potential for further xenograft studies and validated that it maintained *in vitro* sensitivity to BET inhibitor–induced inhibition of cell viability and induction of apoptosis (Supplementary Fig. S5A and S5B). Mice bearing xenograft tumors were then treated daily (including a 1- to 2-day drug holiday per mouse) with subcutaneous administration of vehicle or 30 mg/kg ARV771, a BET PROTAC with confirmed *in vivo* efficacy (56–58). We observed that this treatment regimen was well-tolerated in both cohorts (Supplementary Fig. S5C). Consistent with our *in vitro* data, tumors treated with ARV771 experienced less per-tumor growth over the course of the nearly 3-week treatment (Supplementary Fig. S5D and S5E). These results confirm that ARV771 can attenuate human MPNST cell growth in *in vivo*, as well as *in vitro*, and nominate BET PROTACs for further investigation to improve their pharmacokinetic and pharmacodynamic profile as clinically translatable therapeutic strategies for patients with MPNST with no currently effective treatment options.

Discussion

Advances in therapeutic oncology have enriched patients with multiple options for personalized targeted therapies, but resistance remains a challenge (69, 70). Pathway reactivation is a leading mechanism of resistance to targeted therapies (e.g., inhibitors of BCR-ABL, $BRAF^{V600E}$, MEK, or SMO; refs. 6, 71–73). From these studies emerge a concept that broadly acknowledges the ability of cancer cells to rewire, acquire, or hijack alternative signal transduction pathways to converge on common downstream signaling nodes or oncogenic addictions to sustain tumorigenesis and survival (74–76). Consequently, novel targets or bottlenecks are being actively sought after as alternatives in therapeutic oncology. Among these alternatives, inhibition of chromatin/epigenetic/transcriptional regulators has recently emerged as a promising therapeutic strategy to disarm transcriptional events downstream of oncogenic cell signaling networks in cancer (15–20). Nevertheless, resistance also plagues the promise of this therapeutic strategy. The mechanisms underlying resistance to epigenetic inhibitors, however, are not currently well characterized.

In our studies presented herein, through modeling tumor evolution by studying genetic lesions underlying the development of NF1-associated MPNSTs, we reveal that BRD4 upregulation/addiction is associated with limited sensitivity to BET inhibitors. However, given the requirement for high-dose, single-agent BET inhibitors to efficiently trigger substantial cell death in MPNSTs *in vitro*, and that such high doses are presently difficult to sustain *in vivo*, it is expected that BET inhibitor efficacy will remain limited *in vivo* compared with *in vitro* for many different cancer subtypes under current evaluation in the field. Here, we show that genetic inhibition of BRD4 overcomes resistance to BET inhibitors, thus instigating synthetic lethality *in vitro* and markedly restraining tumor relapse *in vivo* in MPNST. These findings suggest a working model in which strategies to suppress BRD4 expression may lower the dosage of BET inhibitor necessary for *in vivo* MPNST treatment, and therefore improve its therapeutic efficacy. Alternatively, our finding that BET–protein PROTAC treatment surpasses the efficacy of BET inhibitors in cell culture models of MPNST inhibition suggests some BRD4-high tumors may be vulnerable to a PROTAC-based therapeutic strategy to reduce BRD4 levels in MPNST patient tumors.

Although unknown at this time, it may be plausible that BET inhibitor JQ1 exerts off-target effects when BRD4 is depleted. However, several data suggest this is likely not a factor in instigating lethality. First, we observed extreme sensitivity to cell death in BRD4-depleted MPNST cells at low doses of JQ1 (Fig. 1G). Second, additional BET inhibitors including OTX-015, CPI-203, and CPI-0610 had potent effects on BRD4-depleted MPNST cells (similar to JQ1; Fig. 2). Third, although high doses of both JQ1 and OTX-015 (20 μmol/L) induced massive cell death, CPI-203 was unable to do so. Yet, CPI-203 and CPI-0610 were much more potent when BRD4 was depleted in MPNST cells. Altogether, these observations suggest that lethality instigated by BRD4 depletion is not likely to be due to off-target effects. Instead, our data indicate that BET inhibitor therapeutic effects on MPNST cells may be attributed to synthetic lethality caused by additional depletion of BET protein levels.

There are several possible mechanisms whereby this may take place. First, depletion of *Brd4* by CRISPR or shRNA may not completely eliminate all BRD4 proteins from the cell. In this scenario, the remaining BRD4 may then be more acutely sensitive to BET inhibitors, because the inhibitor-to-target stoichiometry has been drastically perturbed. A second possible mechanism for the synthetic lethality we observed is that genetic loss of BRD4 results in a compensatory response by other BET-bromodomain family members such as BRD2 and BRD3, which can also be inhibited by BET inhibitors such as JQ1. Here, depletion of BRD4 would increase cells' dependence on BRD2 or BRD3 function, which subsequent treatment with BET inhibitors would overcome to induce cell death. The possibility of BET-bromodomain family members compensating for one another may explain our observation of a synthetic lethality between sh*BRD3* and JQ1, which displayed a similar, although less potent, phenotype compared to the combination of JQ1 and sh*BRD4*. This mode of compensation would likely occur by increased BRD2/3 function or relative recruitment to acetylated histones rather than by increased BRD2/3 expression, as BRD4 depletion did not correspond to a concomitant increase in BRD3 or BRD2 at the protein level (Supplementary Fig. S2A). A third explanation for the synthetic lethality between BET inhibitors and loss of BRD4 could arise from reported BET bromodomain–dependent and -independent functions of BRD4 (41). In this case, our data would reflect an MPNST cell addiction to the specific activity of the BET bromodomain (sensitive to BET inhibitors) as well as to BET domain–independent functions of BRD4 proteins (sensitive to BRD4 depletion). Finally, BRD4 depletion may counteract possible BET inhibitor–induced feedback upregulation of BRD4 levels or

function. If this explanation underlies our data, then the use of PROTACs, which inhibit BET domain binding to acetylated proteins while simultaneously promoting BRD4 degradation, would be preferable to the use of BET inhibitors alone as a therapeutic strategy.

In conclusion, the elucidation of a link between BET inhibitor efficacy and the cellular level of wild-type BET proteins in MPNST cells provides an important insight into BET inhibitor sensitivity and resistance in cancer cells. This may then provide a framework for developing next-generation inhibitors to overcome resistance and improve the clinical efficacy of this epigenetic therapy. Current and future clinical trials of BET inhibitors in MPNST and other BET-implicated cancers should consider the type of addiction to BET family member proteins such as BRD4 that we report here in assessing future study efficacy. According to our data, we hypothesize that BRD4-high, and accordingly addicted, tumors could benefit from the recent development of small-molecule–targeted protein degraders such as PROTACs or future advances in *in vivo* gene targeting techniques using RNAi. BRD4-low tumors, on the other hand, could be predicted to respond best to strategies using direct BET inhibition alone or in combination with other anticancer agents. These strategies could then be employed in a data-driven manner to provide rational approaches to develop breakthrough treatments for currently therapy-refractory patients with MPNST.

Disclosure of Potential Conflicts of Interest

No potential conflicts of interest were disclosed.

Authors' Contributions

Conception and design: L.Q. Le, J.M. Cooper, A.J. Patel
Development of methodology: L.Q. Le, J.M. Cooper, A.J. Patel, K. Chen, J. Mo
Acquisition of data (provided animals, acquired and managed patients, provided facilities, etc.): L.Q. Le, J.M. Cooper, A.J. Patel, Z. Chen, C.-P. Liao, Y. Wang, J. Mo
Analysis and interpretation of data (e.g., statistical analysis, biostatistics, computational analysis): L.Q. Le, A.J. Patel, J.M. Cooper
Writing, review, and/or revision of the manuscript: L.Q. Le, J.M. Cooper, A.J. Patel
Administrative, technical, or material support (i.e., reporting or organizing data, constructing databases): L.Q. Le, A.J. Patel, Y. Wang, J. Mo
Study supervision: L.Q. Le, A.J. Patel

Acknowledgments

We thank all members of the Le laboratory for helpful suggestions and discussions. We would also like to thank Lili Tao (UTSW, Dallas, TX) and Craig Crews (Yale University, New Haven, CT) for sharing reagents and methodological insights, respectively. A.J. Patel and C.P. Liao were recipients of the Young Investigator Awards from Children's Tumor Foundation. C.P. Liao also receives a Career Development Award from Dermatology Foundation. J.M. Cooper is funded by the Dermatology Research Training Program T32 Grant T32AR065969. L.Q. Le holds a Career Award for Medical Scientists from the Burroughs Wellcome Fund. This work was supported by funding from the Elisabeth Reed Wagner Fund for Research and Clinical Care in Neurofibromatosis and Cardiothoracic Surgery, the Texas Neurofibromatosis Foundation, U.S. Department of Defense grant number W81XWH-14-1-0065, the National Cancer Institute of the NIH grant number R01 CA166593 and Specialized Programs of Research Excellence (SPORE) grant number U54 CA 196519 (to L.Q. Le).

The costs of publication of this article were defrayed in part by the payment of page charges. This article must therefore be hereby marked *advertisement* in accordance with 18 U.S.C. Section 1734 solely to indicate this fact.

Received July 27, 2018; revised December 8, 2018; accepted February 15, 2019; published first February 22, 2019.

References

1. Muller PAJ, Vousden KH. p53 mutations in cancer. Nat Cell Biol 2013;15:2–8.
2. Parada LF, Tabin CJ, Shih C, Weinberg RA. Human EJ bladder carcinoma oncogene is homologue of Harvey sarcoma virus ras gene. Nature 1982;297:474–8.
3. Kufe DWH, James F, Frei Emil III, American Cancer Society. Cancer medicine. Hamilton, Ontario, Canada: BC Decker; 2003.
4. Choi G, Huang B, Pinarbasi E, Braunstein SE, Horvai AE, Kogan S, et al. Genetically mediated Nf1 loss in mice promotes diverse radiation-induced tumors modeling second malignant neoplasms. Cancer Res 2012;72:6425–34.
5. Ris MD, Packer R, Goldwein J, Jones-Wallace D, Boyett JM. Intellectual outcome after reduced-dose radiation therapy plus adjuvant chemotherapy for medulloblastoma: a children's cancer group study. J Clin Oncol 2001;19:3470–6.
6. Nazarian R, Shi H, Wang Q, Kong X, Koya RC, Lee H, et al. Melanomas acquire resistance to B-RAF(V600E) inhibition by RTK or N-RAS upregulation. Nature 2010;468:973–7.
7. Poulikakos PI, Persaud Y, Janakiraman M, Kong X, Ng C, Moriceau G, et al. RAF inhibitor resistance is mediated by dimerization of aberrantly spliced BRAF(V600E). Nature 2011;480:387–90.
8. Shi H, Moriceau G, Kong X, Lee M-K, Lee H, Koya RC, et al. Melanoma whole-exome sequencing identifies V600EB-RAF amplification-mediated acquired B-RAF inhibitor resistance. Nat Commun 2012;3:724.
9. Gschwind A, Fischer OM, Ullrich A. The discovery of receptor tyrosine kinases: targets for cancer therapy. Nat Rev Cancer 2004;4:361–70.
10. Sawyers C. Targeted cancer therapy. Nature 2004;432:294–7.
11. Dijkgraaf GJP, Alicke B, Weinmann L, Januario T, West K, Modrusan Z, et al. Small molecule inhibition of GDC-0449 refractory smoothened mutants and downstream mechanisms of drug resistance. Cancer Res 2011;71:435–44.
12. Johannessen CM, Boehm JS, Kim SY, Thomas SR, Wardwell L, Johnson LA, et al. COT drives resistance to RAF inhibition through MAP kinase pathway reactivation. Nature 2010;468:968–72.
13. Eskiocak U, Kim SB, Ly P, Roig AI, Biglione S, Komurov K, et al. Functional parsing of driver mutations in the colorectal cancer genome reveals numerous suppressors of anchorage-independent growth. Cancer Res 2011;71:4359–65.
14. Wood LD, Parsons DW, Jones S, Lin J, Sjöblom T, Leary RJ, et al. The genomic landscapes of human breast and colorectal cancers. Science 2007;318:1108–13.
15. Dawson Mark A, Kouzarides T. Cancer epigenetics: from mechanism to therapy. Cell 2012;150:12–27.
16. Rius M, Lyko F. Epigenetic cancer therapy: rationales, targets and drugs. Oncogene 2012;31:4257–65.
17. Rodriguez-Paredes M, Esteller M. Cancer epigenetics reaches mainstream oncology. Nat Med 2011:330–9.
18. Shortt J, Ott CJ, Johnstone RW, Bradner JE. A chemical probe toolbox for dissecting the cancer epigenome. Nat Rev Cancer 2017;17:160–83.
19. Fujisawa T, Filippakopoulos P. Functions of bromodomain-containing proteins and their roles in homeostasis and cancer. Nat Rev Mol Cell Biol 2017;18:246–62.
20. Stathis A, Bertoni F. BET proteins as targets for anticancer treatment. Cancer Discov 2018;8:24–36.
21. De Carvalho Daniel D, Sharma S, You Jueng S, Su S-F, Taberlay Phillippa C, Kelly Theresa K, et al. DNA methylation screening identifies driver epigenetic events of cancer cell survival. Cancer Cell 2012;21:655–67.
22. Hu X, Feng Y, Zhang D, Zhao Sihai D, Hu Z, Greshock J, et al. A functional genomic approach identifies FAL1 as an oncogenic long noncoding RNA that associates with BMI1 and represses p21 expression in cancer. Cancer Cell 2014;26:344–57.

23. Lee W, Teckie S, Wiesner T, Ran L, Prieto Granada CN, Lin M, et al. PRC2 is recurrently inactivated through EED or SUZ12 loss in malignant peripheral nerve sheath tumors. Nat Genet 2014;46:1227–32.
24. Lian Christine G, Xu Y, Ceol C, Wu F, Larson A, Dresser K, et al. Loss of 5-Hydroxymethylcytosine is an epigenetic hallmark of melanoma. Cell 2012;150:1135–46.
25. Wang GG, Allis CD, Chi P. Chromatin remodeling and cancer, part I: covalent histone modifications. Trends Mol Med 2007;13:363–72.
26. Wang GG, Allis CD, Chi P. Chromatin remodeling and cancer, part II: ATP-dependent chromatin remodeling. Trends Mol Med 2007;13:373–80.
27. Yamazaki H, Suzuki M, Otsuki A, Shimizu R, Bresnick Emery H, Engel James D, et al. A remote GATA2 hematopoietic enhancer drives leukemogenesis in inv(3)(q21;q26) by activating EVI1 expression. Cancer Cell 2014;25:415–27.
28. Riveiro ME, Astorgues-Xerri L, Vazquez R, Frapolli R, Kwee I, Rinaldi A, et al. OTX015 (MK-8628), a novel BET inhibitor, exhibits antitumor activity in non-small cell and small cell lung cancer models harboring different oncogenic mutations. Oncotarget 2016;7:84675–87.
29. Alsarraj J, Walker RC, Webster JD, Geiger TR, Crawford NPS, Simpson RM, et al. Deletion of the proline-rich region of the murine metastasis susceptibility gene Brd4 promotes epithelial-to-mesenchymal transition- and stem cell-like conversion. Cancer Res 2011;71:3121–31.
30. Asangani IA, Dommeti VL, Wang X, Malik R, Cieslik M, Yang R, et al. Therapeutic targeting of BET bromodomain proteins in castration-resistant prostate cancer. Nature 2014;510:278–82.
31. Dawson MA, Prinjha RK, Dittmann A, Giotopoulos G, Bantscheff M, Chan W-I, et al. Inhibition of BET recruitment to chromatin as an effective treatment for MLL-fusion leukaemia. Nature 2011;478:529–33.
32. Delmore Jake E, Issa Ghayas C, Lemieux Madeleine E, Rahl Peter B, Shi J, Jacobs Hannah M, et al. BET bromodomain inhibition as a therapeutic strategy to target c-Myc. Cell 2011;146:904–17.
33. Filippakopoulos P, Qi J, Picaud S, Shen Y, Smith WB, Fedorov O, et al. Selective inhibition of BET bromodomains. Nature 2010;468:1067–73.
34. Patel Amish J, Liao C-P, Chen Z, Liu C, Wang Y, Le Lu Q. BET bromodomain inhibition triggers apoptosis of NF1-associated malignant peripheral nerve sheath tumors through bim induction. Cell Rep 2014;6:81–92.
35. Segura MF, Fontanals-Cirera B, Gaziel-Sovran A, Guijarro MV, Hanniford D, Zhang G, et al. BRD4 sustains melanoma proliferation and represents a new target for epigenetic therapy. Cancer Res 2013;73:6264–76.
36. Zuber J, Shi J, Wang E, Rappaport AR, Herrmann H, Sison EA, et al. RNAi screen identifies Brd4 as a therapeutic target in acute myeloid leukaemia. Nature 2011;478:524–8.
37. Henssen A, Althoff K, Odersky A, Beckers A, Koche R, Speleman F, et al. Targeting MYCN-driven transcription by BET-bromodomain inhibition. Clin Cancer Res 2016;22:2470–81.
38. Wu SY, Chiang CM. The double bromodomain-containing chromatin adaptor Brd4 and transcriptional regulation. J Biol Chem 2007;282:13141–5.
39. Wu SY, Lee AY, Lai HT, Zhang H, Chiang CM. Phospho switch triggers Brd4 chromatin binding and activator recruitment for gene-specific targeting. Mol Cell 2013;49:843–57.
40. Kurimchak AM, Shelton C, Duncan KE, Johnson KJ, Brown J, O'Brien S, et al. Resistance to BET bromodomain inhibitors is mediated by kinome reprogramming in ovarian cancer. Cell Rep 2016;16:1273–86.
41. Shu S, Lin CY, He HH, Witwicki RM, Tabassum DP, Roberts JM, et al. Response and resistance to BET bromodomain inhibitors in triple-negative breast cancer. Nature 2016;529:413–7.
42. Rathert P, Roth M, Neumann T, Muerdter F, Roe JS, Muhar M, et al. Transcriptional plasticity promotes primary and acquired resistance to BET inhibition. Nature 2015;525:543–7.
43. Fong CY, Gilan O, Lam EY, Rubin AF, Ftouni S, Tyler D, et al. BET inhibitor resistance emerges from leukaemia stem cells. Nature 2015;525:538–42.
44. Chapuy B, McKeown Michael R, Lin Charles Y, Monti S, Roemer Margaretha GM, Qi J, et al. Discovery and characterization of super-enhancer-associated dependencies in diffuse large B cell lymphoma. Cancer Cell 2013;24:777–90.
45. Lovén J, Hoke Heather A, Lin Charles Y, Lau A, Orlando David A, Vakoc Christopher R, et al. Selective inhibition of tumor oncogenes by disruption of super-enhancers. Cell 2013;153:320–34.
46. Shi J, Whyte WA, Zepeda-Mendoza CJ, Milazzo JP, Shen C, Roe J-S, et al. Role of SWI/SNF in acute leukemia maintenance and enhancer-mediated Myc regulation. Genes Dev 2013;27:2648–62.
47. Amorim S, Stathis A, Gleeson M, Iyengar S, Magarotto V, Leleu X, et al. Bromodomain inhibitor OTX015 in patients with lymphoma or multiple myeloma: a dose-escalation, open-label, pharmacokinetic, phase 1 study. Lancet Haematol 2016;3:e196–204.
48. Berthon C, Raffoux E, Thomas X, Vey N, Gomez-Roca C, Yee K, et al. Bromodomain inhibitor OTX015 in patients with acute leukaemia: a dose-escalation, phase 1 study. Lancet Haematol 2016;3:e186–95.
49. King B, Trimarchi T, Reavie L, Xu L, Mullenders J, Ntziachristos P, et al. The ubiquitin ligase FBXW7 modulates leukemia-initiating cell activity by regulating MYC stability. Cell 2013;153:1552–66.
50. Chau V, Lim SK, Mo W, Liu C, Patel AJ, McKay RM, et al. Preclinical therapeutic efficacy of a novel pharmacologic inducer of apoptosis in malignant peripheral nerve sheath tumors. Cancer Res 2014;74:586–97.
51. Mo W, Chen J, Patel A, Zhang L, Chau V, Li Y, et al. CXCR4/CXCL12 mediate autocrine cell- cycle progression in NF1-associated malignant peripheral nerve sheath tumors. Cell 2013;152:1077–90.
52. Zhang M, Wang Y, Jones S, Sausen M, McMahon K, Sharma R, et al. Somatic mutations of SUZ12 in malignant peripheral nerve sheath tumors. Nat Genet 2014;46:1170–2.
53. De Raedt T, Beert E, Pasmant E, Luscan A, Brems H, Ortonne N, et al. PRC2 loss amplifies Ras-driven transcription and confers sensitivity to BRD4-based therapies. Nature 2014;514:247–51.
54. Brohl AS, Kahen E, Yoder SJ, Teer JK, Reed DR. The genomic landscape of malignant peripheral nerve sheath tumors: diverse drivers of Ras pathway activation. Sci Rep 2017;7:14992.
55. Conery AR, Centore RC, Spillane KL, Follmer NE, Bommi-Reddy A, Hatton C, et al. Preclinical anticancer efficacy of BET bromodomain inhibitors is determined by the apoptotic response. Cancer Res 2016;76:1313–9.
56. Raina K, Lu J, Qian Y, Altieri M, Gordon D, Rossi AM, et al. PROTAC-induced BET protein degradation as a therapy for castration-resistant prostate cancer. Proc Natl Acad Sci U S A 2016;113:7124–9.
57. Sun B, Fiskus W, Qian Y, Rajapakshe K, Raina K, Coleman KG, et al. BET protein proteolysis targeting chimera (PROTAC) exerts potent lethal activity against mantle cell lymphoma cells. Leukemia 2018;32:343–52.
58. Saenz DT, Fiskus W, Manshouri T, Rajapakshe K, Krieger S, Sun B, et al. BET protein bromodomain inhibitor-based combinations are highly active against post-myeloproliferative neoplasm secondary AML cells. Leukemia 2017;31:678–87.
59. Ran FA, Hsu PD, Wright J, Agarwala V, Scott DA, Zhang F. Genome engineering using the CRISPR-Cas9 system. Nat Protoc 2013;8:2281–308.
60. Wang T, Wei JJ, Sabatini DM, Lander ES. Genetic screens in human cells using the CRISPR-Cas9 system. Science 2014;343:80–4.
61. Cooper JM, Ou YH, McMillan EA, Vaden RM, Zaman A, Bodemann BO, et al. TBK1 provides context-selective support of the activated AKT/mTOR pathway in lung cancer. Cancer Res 2017;77:5077–94.
62. Knoechel B, Roderick JE, Williamson KE, Zhu J, Lohr JG, Cotton MJ, et al. An epigenetic mechanism of resistance to targeted therapy in T cell acute lymphoblastic leukemia. Nat Genet 2014;46:364–70.
63. Filippakopoulos P, Knapp S. Targeting bromodomains: epigenetic readers of lysine acetylation. Nat Rev Drug Discov 2014;13:337–56.
64. Riggs DL, Chesi M, Bergsagel PL. Targeting MYC in multiple myeloma by BET protein inhibition. Cancer Res 2014;74:5489-.
65. Albrecht BK, Gehling VS, Hewitt MC, Vaswani RG, Cote A, Leblanc Y, et al. Identification of a benzoisoxazoloazepine inhibitor (CPI-0610) of the Bromodomain and Extra-Terminal (BET) family as a candidate for human clinical trials. J Med Chem 2016;59:1330–9.
66. Lai AC, Crews CM. Induced protein degradation: an emerging drug discovery paradigm. Nat Rev Drug Discov 2017;16:101–14.
67. Lu J, Qian Y, Altieri M, Dong H, Wang J, Raina K, et al. Hijacking the E3 ubiquitin ligase cereblon to efficiently target BRD4. Chem Biol 2015;22:755–63.
68. Bondeson DP, Mares A, Smith IE, Ko E, Campos S, Miah AH, et al. Catalytic in vivo protein knockdown by small-molecule PROTACs. Nat Chem Biol 2015;11:611–7.

69. Hamburg MA, Collins FS. The path to personalized medicine. N Engl J Med 2010;363:301–4.
70. Tursz T, re F, Lazar V, Lacroix L, Soria J-C. Implications of personalized medicine[mdash]perspective from a cancer center. Nat Rev Clin Oncol 2011;8:177–83.
71. Corcoran Ryan B, Cheng Katherine A, Hata Aaron N, Faber Anthony C, Ebi H, Coffee Erin M, et al. Synthetic lethal interaction of combined BCL-XL and MEK inhibition promotes tumor regressions in KRAS mutant cancer models. Cancer Cell 2013;23:121–8.
72. Ma L, Shan Y, Bai R, Xue L, Eide CA, Ou J, et al. A therapeutically targetable mechanism of BCR-ABL–independent imatinib resistance in chronic myeloid leukemia. Sci Transl Med 2014;6:252ra121.
73. Zabriskie Matthew S, Eide Christopher A, Tantravahi Srinivas K, Vellore Nadeem A, Estrada J, Nicolini Franck E, et al. BCR-ABL1 compound mutations combining key kinase domain positions confer clinical resistance to ponatinib in Ph Chromosome-positive leukemia. Cancer Cell 2014;26:428–42.
74. Dail M, Wong J, Lawrence J, O/'Connor D, Nakitandwe J, Chen S-C, et al. Loss of oncogenic Notch1 with resistance to a PI3K inhibitor in T-cell leukaemia. Nature 2014;513:512–6.
75. Garraway LA, Jänne PA. Circumventing cancer drug resistance in the era of personalized medicine. Cancer Discov 2012;2:214–26.
76. Holohan C, Van Schaeybroeck S, Longley DB, Johnston PG. Cancer drug resistance: an evolving paradigm. Nat Rev Cancer 2013;13:714–26.